

Quantum Monte Carlo Study of the Two-Dimensional Homogeneous Electron Gas

Neil D. Drummond and Richard J. Needs

TCM Group, Cavendish Laboratory, University of Cambridge

*Quantum Monte Carlo in the Apuan Alps IV
TTI, Vallico Sotto, Italy*

Tuesday 29th July, 2008

Two-Dimensional Homogeneous Electron Gas (I)

- **2D HEG**: set of electrons moving in 2D in a uniform, inert, neutralising background.
- Hamiltonian (for finite system):

$$\hat{H} = \sum_i -\frac{1}{2}\nabla_i^2 + \sum_{j>i} v_E(\mathbf{r}_{ij}) + \frac{Nv_M}{2}.$$

Infinite-system GS energy per particle depends only on the **density** (specified by radius r_s of circle containing one electron on average) and **spin polarisation** [$\zeta = (N_\uparrow - N_\downarrow)/N$].

- Physical realisations:
 - *Electrons on metal surfaces*. E.g. Cu [111].
 - *Electrons on droplets of liquid He*. Held in place by image charges
 - *Inversion layers in MOS devices*. Can easily tune density. Electrons far from dopants; fewer complications due to disorder; technologically important.

Two-Dimensional Homogeneous Electron Gas (II)

- HEG is simplest fully interacting quantum many-body system.
- QMC is the only accurate method available for studying its ground-state properties.
- We have carried out QMC studies of the 2D HEG:
 1. We have calculated the zero-temperature phase diagram.¹
 2. We have calculated the PCF, structure factor and momentum distribution.²
 3. We are currently calculating the single-particle energy band and hence quasiparticle effective mass.
- Our data will hopefully be of interest to
 - Experimentalists looking for ferromagnetism and Wigner crystallisation in low-density 2D HEGs.
 - Theorists interested in constructing 2D XC functionals for DFT calculations.

¹ N. D. Drummond and R. J. Needs, submitted to Phys. Rev. Lett. (2008).

² N. D. Drummond and R. J. Needs, submitted to Phys. Rev. B (2008).

Wigner Crystallisation in 2D (I)

- Kinetic energy dominates at high density: *form Fermi fluid to minimise it.*
- Potential energy dominates at low density: *form Wigner crystal to minimise it.*
- Wigner crystals have been observed on the surface of liquid helium³ and in inversion layers in MOSFET devices⁴.
- 2D Wigner crystals could be of use in quantum computing devices.⁵
- Previous QMC studies⁶ indicate that fluid–crystal transition occurs somewhere between $r_s = 25$ and 40 a.u.
- Can we be more precise?

³ C. C. Grimes and G. Adams, Phys. Rev. Lett. **42**, 795 (1979).

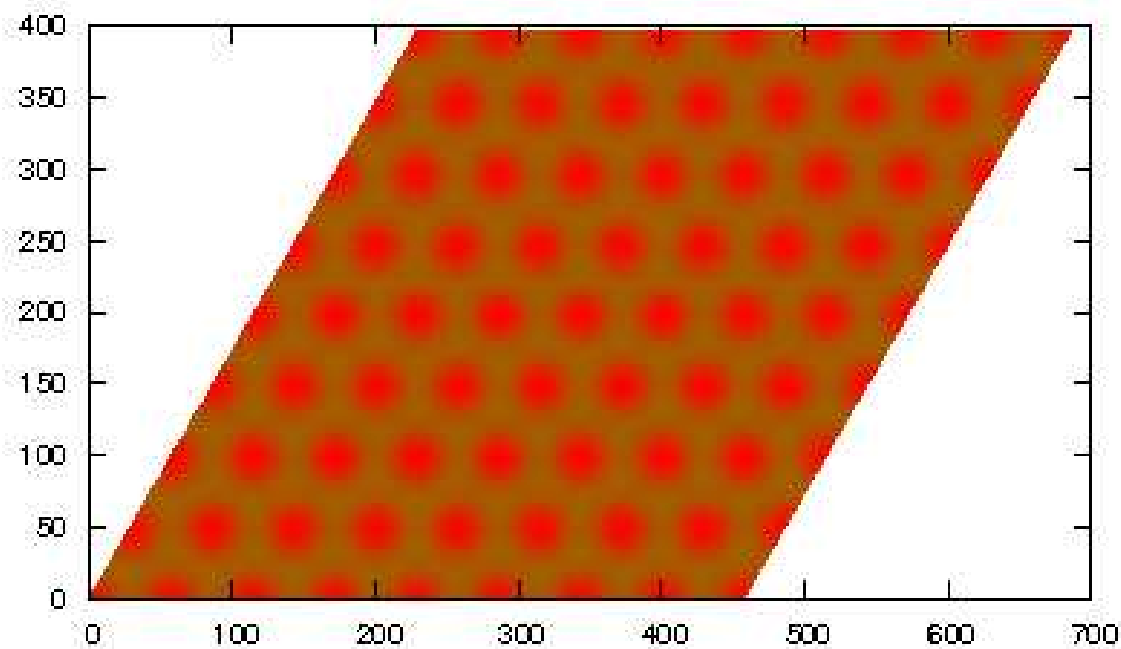
⁴ E. Y. Andrei *et al.*, Phys. Rev. Lett. **60**, 2765 (1988); R. L. Willett *et al.*, Phys. Rev. B **38**, 7881 (1988).

⁵ P. M. Platzman & M. I. Dykman, Science **284**, 1967 (1999); P. Glasson *et al.*, Phys. Rev. Lett. **87**, 176802 (2001).

⁶ B. Tanatar & D. M. Ceperley, Phys. Rev. B **39**, 5005 (1989); F. Rapisarda & G. Senatore, Aust. J. Phys. **49**, 161 (1996).

Wigner Crystallisation in 2D (II)

- Triangular lattice has lowest Madelung constant. Wins at low density.
- Hartree–Fock theory⁷: antiferromagnetic square lattice \rightarrow ferromagnetic triangular lattice at $r_s = 2.6$ a.u.
- We consider only triangular lattices.



⁷ J. R. Trail, M. D. Towler and R. J. Needs, Phys. Rev. B **68**, 045107 (2003).

Magnetic Behaviour of the Fermi Fluid

- Bloch transition: para. fluid favoured at high density (want to minimise KE); ferro. fluid favoured at low density (keep electrons apart to minimise XC energy).
- **Hartree–Fock theory**: Bloch transition at $r_s = 2.01$ a.u. No region of stability for ferromagnetic fluid.
- **VMC**⁸: Bloch transition at $r_s = 13(2)$ a.u.; crystallisation at $r_s = 33(2)$ a.u.
- **DMC**⁹: Bloch and crystallisation transitions at $r_s = 37(5)$ a.u.
- **DMC**¹⁰: Bloch transition at $r_s = 20(2)$ a.u. and crystallisation at $r_s = 34(4)$ a.u.
- **Experiment**¹¹: “Possible evidence” of ferromagnetism at $r_s = 7.6$ a.u.

⁸ D. Ceperley, Phys. Rev. B **18**, 3126 (1978).

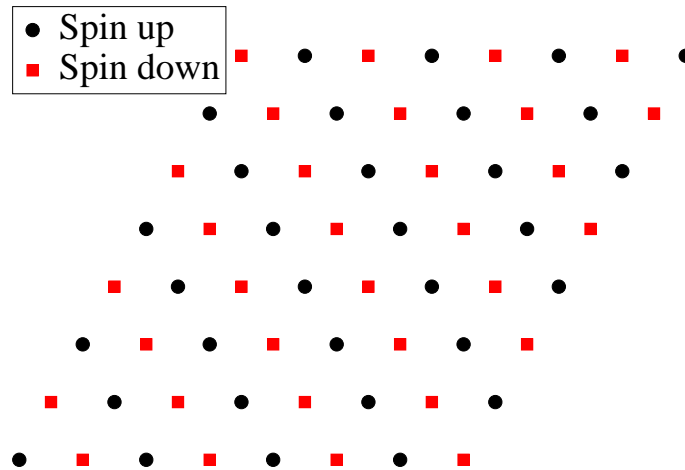
⁹ B. Tanatar and D. M. Ceperley, Phys. Rev. B **39**, 5005 (1989).

¹⁰ F. Rapisarda and G. Senatore, Aust. J. Phys. **49**, 161 (1996).

¹¹ A. Ghosh, C. J. B. Ford, M. Pepper, H. E. Beere and D. A. Ritchie, Phys. Rev. Lett. **92**, 116601 (2004).

Magnetic Behaviour of the Wigner Crystal

- Hartree-Fock theory¹²: ferromagnetic for $r_s > 2.6$ a.u.
- Multispin exchange model¹³: frustrated antiferromagnetism (spin liquid) → ferromagnetism at $r_s = 175(10)$ a.u.
- We have studied both ferromagnetic and antiferromagnetic triangular crystals.
- We have used striped antiferromagnetic crystals. Energy should be close to that of the spin liquid.



¹² J. R. Trail, M. D. Towler and R. J. Needs, Phys. Rev. B **68**, 045107 (2003).

¹³ B. Bernu, L. Candido and D. M. Ceperley, Phys. Rev. Lett. **86**, 873 (2001).

Fermi Fluid: PBC, TBC and TABC

- Orbitals for Fermi fluid:

$$\phi_{\mathbf{k}}(\mathbf{r}) = \exp(i\mathbf{k} \cdot \mathbf{r}).$$

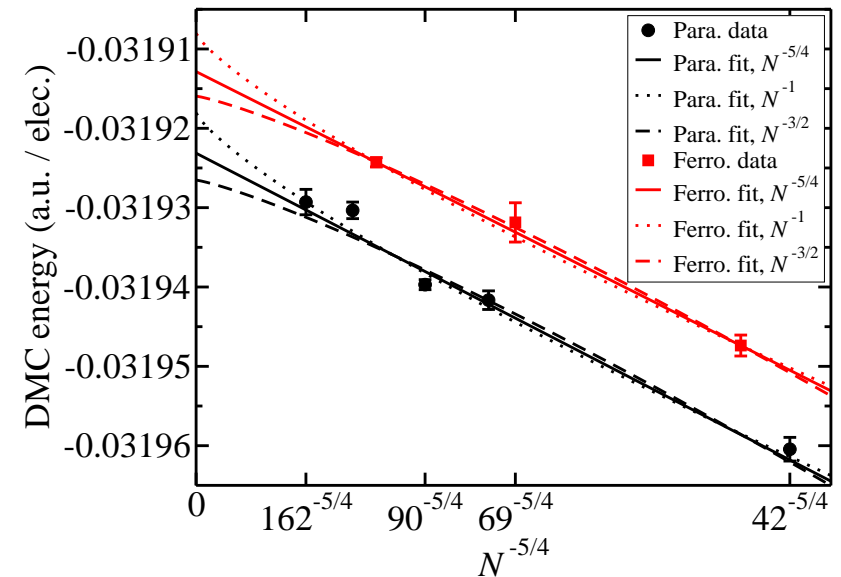
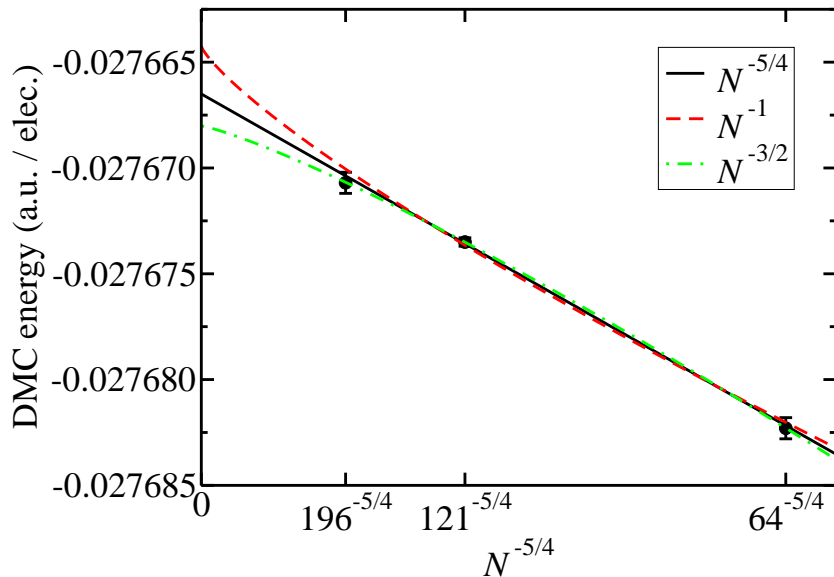
- **Periodic boundary conditions:** $\{\mathbf{k}\}$ are simulation-cell \mathbf{G} -vectors.
- **Single-particle finite-size effects:** Increase N at fixed density; grid of \mathbf{G} -vectors gets finer; energy per electron jumps as shells of \mathbf{G} vectors pass through Fermi line.
- **Twisted boundary conditions:** \mathbf{k} are simulation-cell \mathbf{G} vectors offset by $\mathbf{k}_s \in 1\text{st BZ}$ of simulation cell.
- **Twist averaging:** average over all \mathbf{k}_s . Replaces grid of \mathbf{k} by a Fermi area (equal to area of Fermi circle), greatly reducing single-particle finite-size effects. Shape of Fermi line isn't quite right: gives negligibly small positive bias to KE.
- Previous QMC studies of 2D HEG have not used twist averaging.

Long-Ranged Finite-Size Errors

- Compression of XC hole and neglect of long-ranged two-body correlations in finite cell give error in 2D energy per electron going as $\mathcal{O}(N^{-5/4})$.¹⁴ Extrapolate using:

$$E_N = E_\infty - bN^{-5/4}.$$

- Previous QMC studies have used $N^{-3/2}$ for crystals and N^{-1} for fluid.



Left: crystal extrapolation at $r_s = 35$ a.u.; right: fluid extrapolation at $r_s = 30$ a.u.

¹⁴ N. D. Drummond, R. J. Needs, A. Sorouri and W. M. C. Foulkes, submitted to Phys. Rev. B.

Backflow Transformation

- Evaluate Slater wave function at quasiparticle coordinates related to actual electron coordinates by electron–electron backflow functions.¹⁵
- Moves nodal surface of wave function; can improve the fixed-node DMC energy.
- BF is more significant in fluids than crystals, where electrons are already kept apart by localisation on lattice sites.
- Parallel spins are already kept away from each other by wave-function antisymmetry. BF is much less important in ferromagnetic systems.

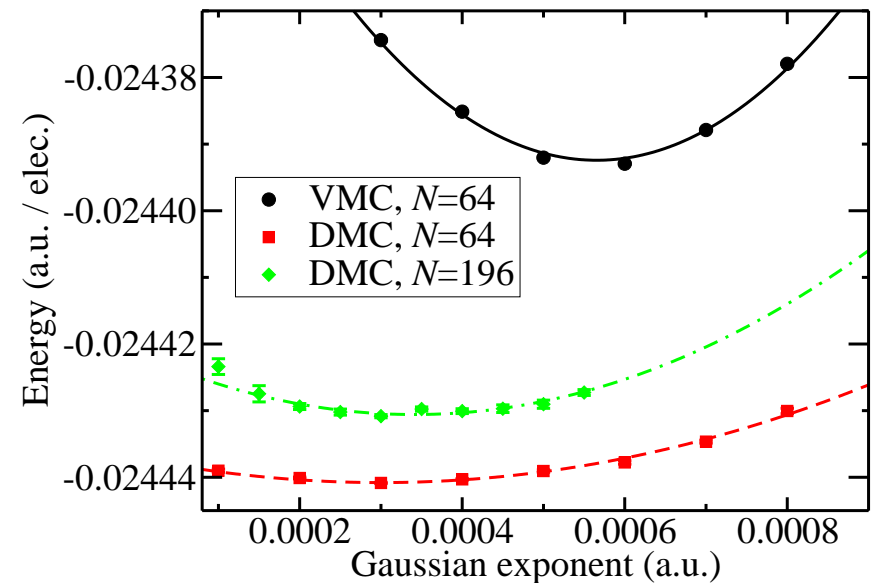
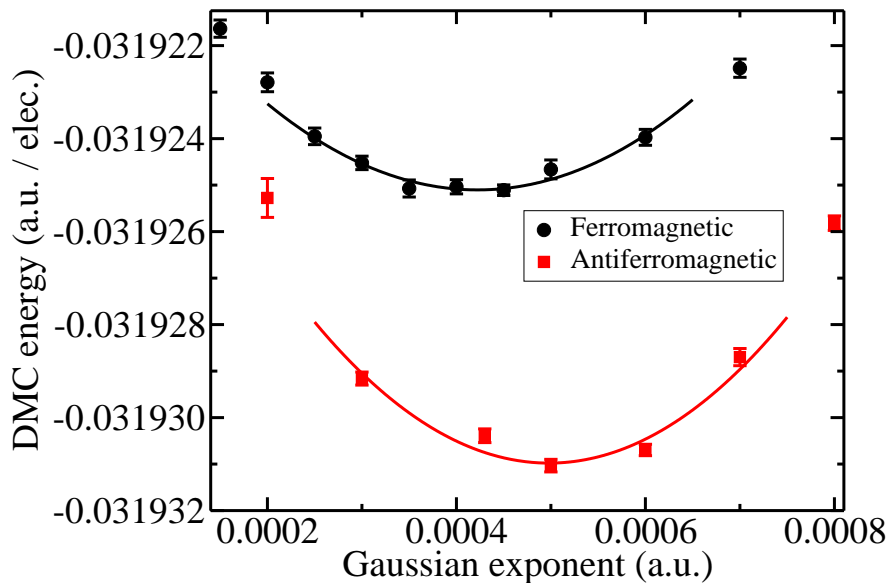
System ($r_s = 30$ a.u.)	Lowering of energy due to BF ($\mu\text{Ha} / \text{elec.}$)
Paramagnetic fluid	36(3)
Ferromagnetic fluid	1.5(4)
Antiferromagnetic crystal	6(1)
Ferromagnetic crystal	1.0(4)

¹⁵ P. López Ríos, A. Ma, N. D. Drummond, M. D. Towler and R. J. Needs, Phys. Rev. E **74**, 066701 (2006).

Optimisation of Crystal Orbitals

Crystal orbitals: $\phi_{\mathbf{R}}(\mathbf{r}) = \exp(-C|\mathbf{r} - \mathbf{R}|^2)$.

Only orbital parameter affecting crystal nodal surface: Gaussian exponent C . Minimise DMC energy w.r.t. C to minimise fixed-node error.



DMC energy against C at $r_s = 30$ a.u. (left) and $r_s = 40$ a.u. (right) (ferro. crystals).

Ferromagnetic crystals: optimal exponent is $C_{\text{DMC}}^{\text{F}} = 0.071r_s^{-3/2}$.

(CF, VMC exponent is $C_{\text{VMC}}^{\text{F}} = 0.15r_s^{-3/2}$ and HF exponent is $C_{\text{HF}}^{\text{F}} = 0.46r_s^{-3/2}$.)

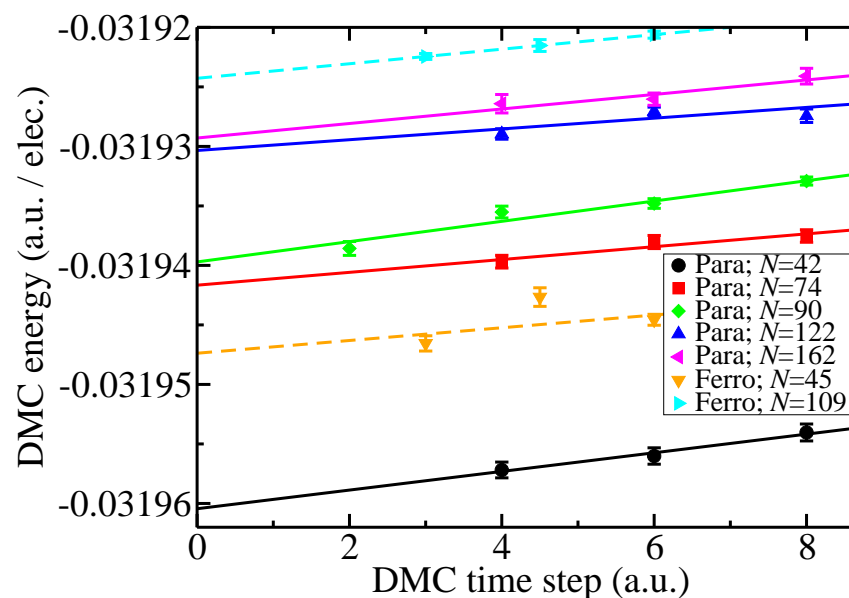
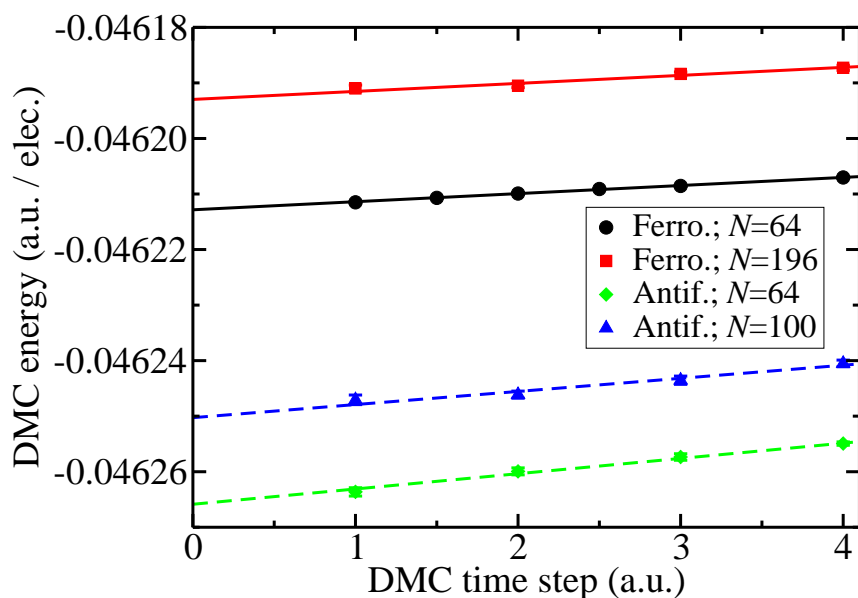
Antiferromagnetic crystals: optimal exponent is $C_{\text{DMC}}^{\text{AF}} = 0.082r_s^{-3/2}$.

Time-Step and Population-Control Biases

Population-control bias is bad at low density.¹⁶

Use about 1600 configurations to make population-control bias negligible.

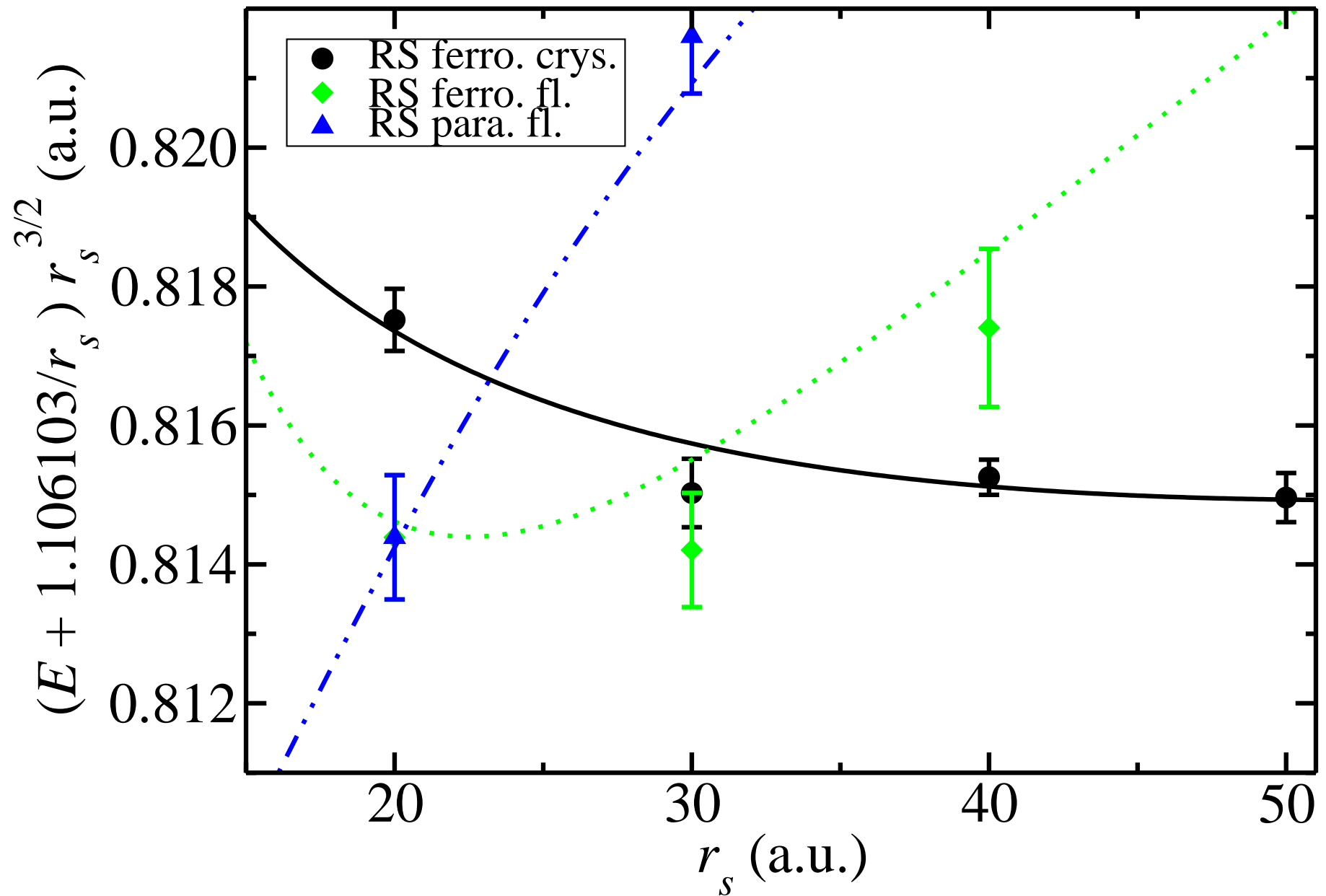
Time-step bias is linear; extrapolate DMC energies to zero time step.



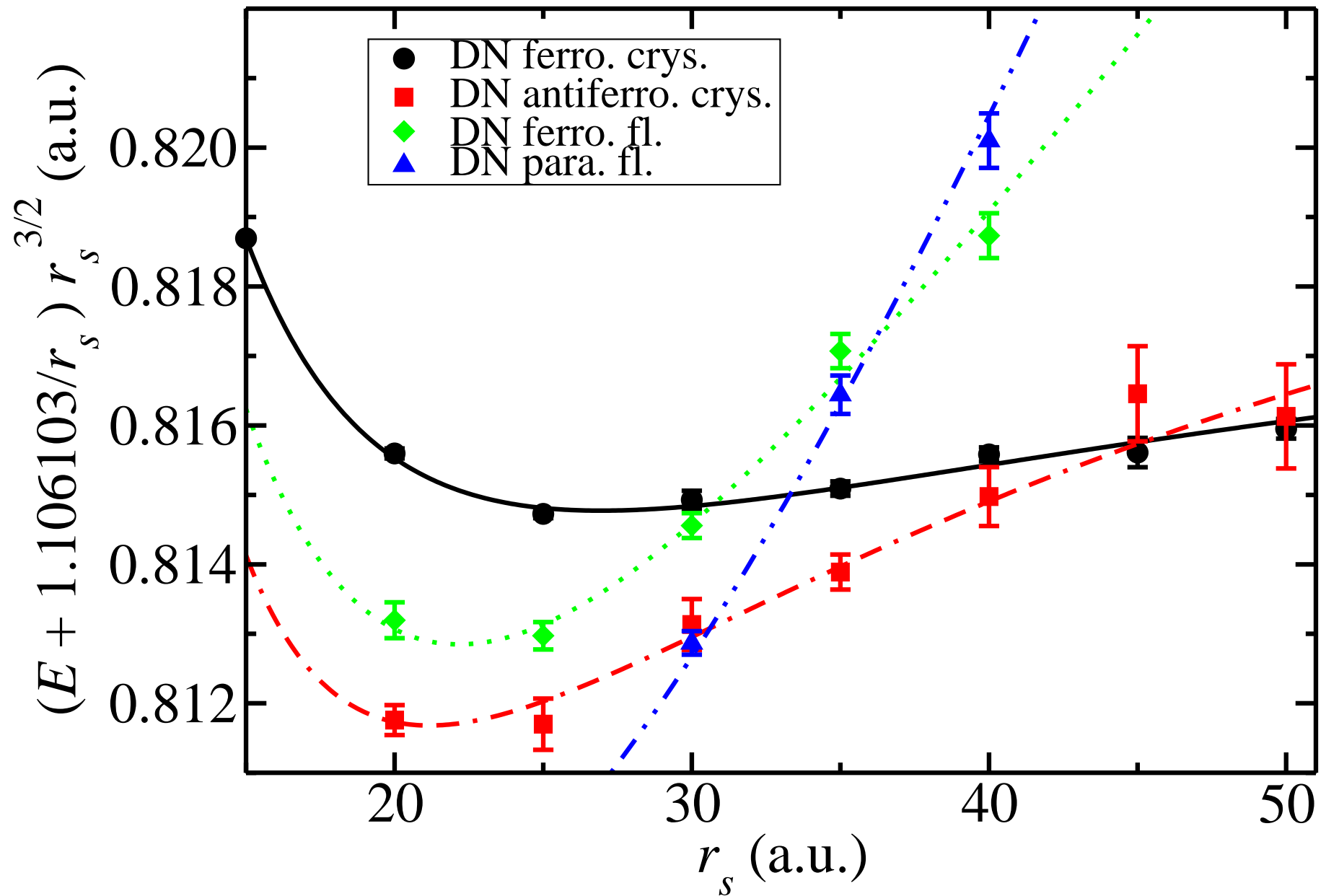
DMC energy against time step for a ferromagnetic crystal at $r_s = 20$ a.u. (left) and fluid at $r_s = 30$ a.u. (right).

¹⁶ N. D. Drummond, Z. Radnai, J. R. Trail, M. D. Towler and R. J. Needs, Phys. Rev. B **69**, 085116 (2004).

2D HEG Energy Diagram (I)



2D HEG Energy Diagram (I)



2D HEG Energy Diagram (II)

- Fully polarised fluid is never stable.
- Wigner crystallisation occurs at $r_s = 30 \pm 1$ a.u. Transition is from a **paramagnetic fluid** to an **antiferromagnetic Wigner crystal**.
- Further transition: **antiferromagnetic** \rightarrow **ferromagnetic** crystal at $r_s = 45 \pm 5$ a.u.
- At $r_s = 35$ a.u., the energy of a fluid with $\zeta = 2/5$ agrees with the paramagnetic and ferromagnetic fluid energies. Very unlikely that a region of stability for a partially polarised fluid exists.
- Phase transitions in 2D HEG cannot be first order.¹⁷
- It's energetically favourable to form boundaries between macroscopically separated phases, so a “microemulsion” is formed at crystallisation density.
- New phases could “round off corners” in energy diagram.

¹⁷ B. Spivak and S. A. Kivelson, Phys. Rev. B **70**, 155114 (2004); R. Jamei *et al.*, Phys. Rev. Lett. **94**, 056805 (2005).

Hybrid Phases (I)

- It's been suggested that there exist **hybrid** phases that are neither fluid nor crystal¹⁸. Orbitals are long-ranged Wannier functions. (From limit that band-gap closes.)
- Have tried using orbitals of the form

$$\phi_{\mathbf{R}}(\mathbf{r}) = \exp(-C|\mathbf{r} - \mathbf{R}|^2) + \sum_S c_S \sum_{\mathbf{G} \in S} \cos[\mathbf{G} \cdot (\mathbf{r} - \mathbf{R})],$$

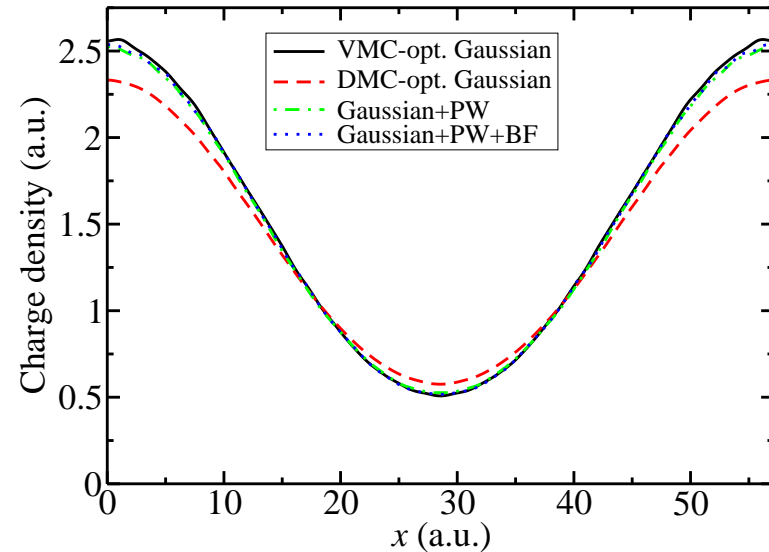
where C and the c_S are optimisable. S runs over stars of \mathbf{G} vectors. This form of orbital can describe the proposed hybrid phase and the crystal phase, but not the fluid phase (which is a partially filled band).

- Tried variance and energy minimisation, brute force VMC, and brute force DMC optimisation, starting from both $c_P = 0$ and random $\{c_P\}$. Tried fixed and free Gaussian exponent C .
- Restricted ourselves to ferromagnetic phases.

¹⁸ H. Falakshahi and X. Waintal, Phys. Rev. Lett. **94**, 046801 (2005); X. Waintal, Phys. Rev. B **73**, 075417 (2006).

Hybrid Phases (II)

Method	Orbitals	BF	Energy (a.u. / elec.)
VMC	DMC-opt. Gauss.+PW	No	-0.031 838 45(5)
VMC	DMC-opt. Gauss.	No	-0.031 840 13(3)
VMC	VMC-opt. Gauss.	No	-0.031 850 15(9)
VMC	Gauss.+PW	No	-0.031 852 97(7)
VMC	Gauss.+PW	Yes	-0.031 871 3(1)
DMC	VMC-opt. Gauss.	No	-0.031 916 5(3)
DMC	Gauss.+PW	No	-0.031 917 9(3)
DMC	Gauss.+PW	Yes	-0.031 918 0(3)
DMC	DMC-opt. Gauss.	No	-0.031 919 7(2)
DMC	DMC-opt. Gauss.+PW	No	-0.031 919 9(5)



- Can lower VMC energy slightly with hybrid wave function.
- Doesn't change charge density (optimising exponent in DMC has a greater effect).
- Doesn't lower DMC energy as much as optimising Gaussian exponent within DMC.
- Suggests we aren't really finding a new phase.

Contact PCF of Paramagnetic Fluid (I)

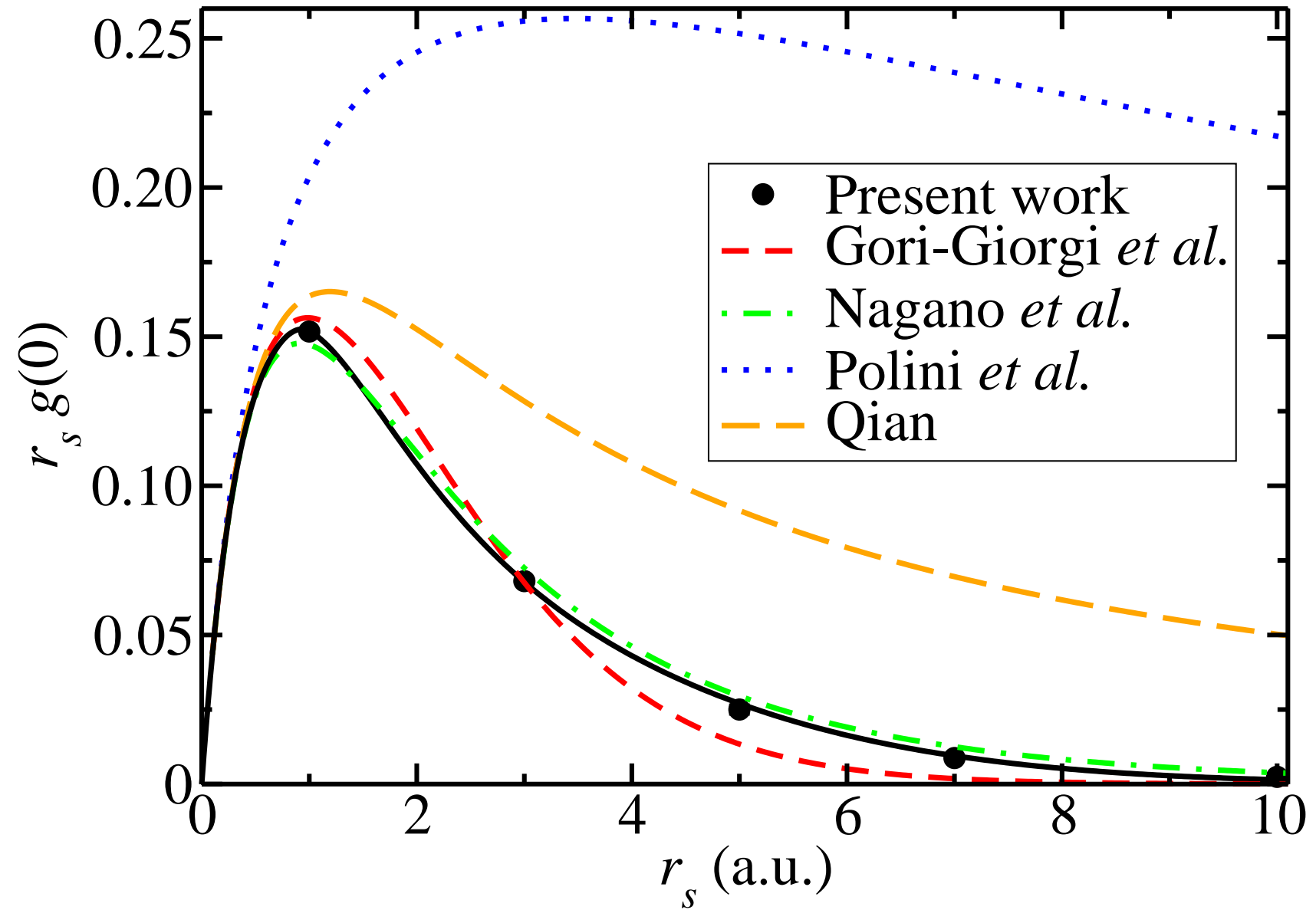
- $g(0)$ is an important parameter in construction of GGA XC functionals.
- Most theoretical calculations of $g(0)$ have used *ladder theory* to solve approximately the Bethe–Goldstone equation for the effective interaction between two electrons. Exact in high-density limit, but not at low densities.
- Disagreement between old approximation¹⁹ in ladder theory and a better approximation,²⁰ and between the better approximation in ladder theory and QMC.²¹
Which is right?
- We evaluate $g(r)$ [including $g(0)$] by binning interparticle distances. Easier in 2D than 3D. Easier at high density than low density.
- Earlier study used Slater–Jastrow wave function and no twist averaging; ours used Slater–Jastrow–**backflow** wave functions and **twist averaging**.

¹⁹ S. Nagano, K. S. Singwi, and S. Ohnishi, Phys. Rev. B **29**, 1209 (1984); *Erratum*, Phys. Rev. B **31**, 3166 (1985).

²⁰ Z. Qian, Phys. Rev. B **73**, 035106 (2006).

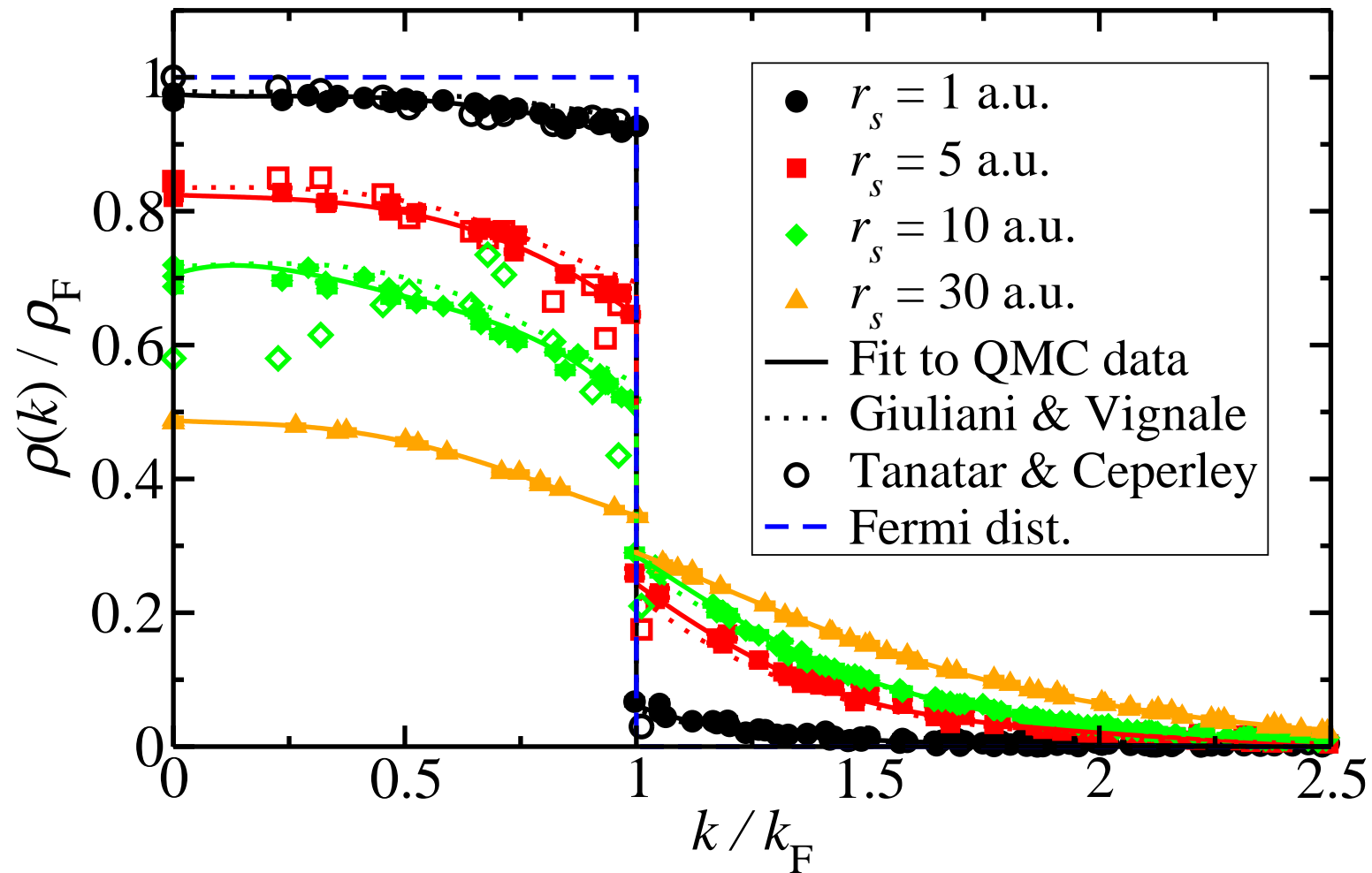
²¹ P. Gori-Giorgi, S. Moroni, and G. B. Bachelet, Phys. Rev. B **70**, 115102 (2004).

Contact PCF of Paramagnetic Fluid (II)



Momentum Density of Paramagnetic Fluid

Discontinuity at Fermi edge is important in Fermi liquid theory. Old QMC data²² shows rise in MD at Fermi edge at low density. Our new data doesn't show this.



²² B. Tanatar and D. M. Ceperley, Phys. Rev. B **39**, 5005 (1989).

Single-Particle Energy Band (I)

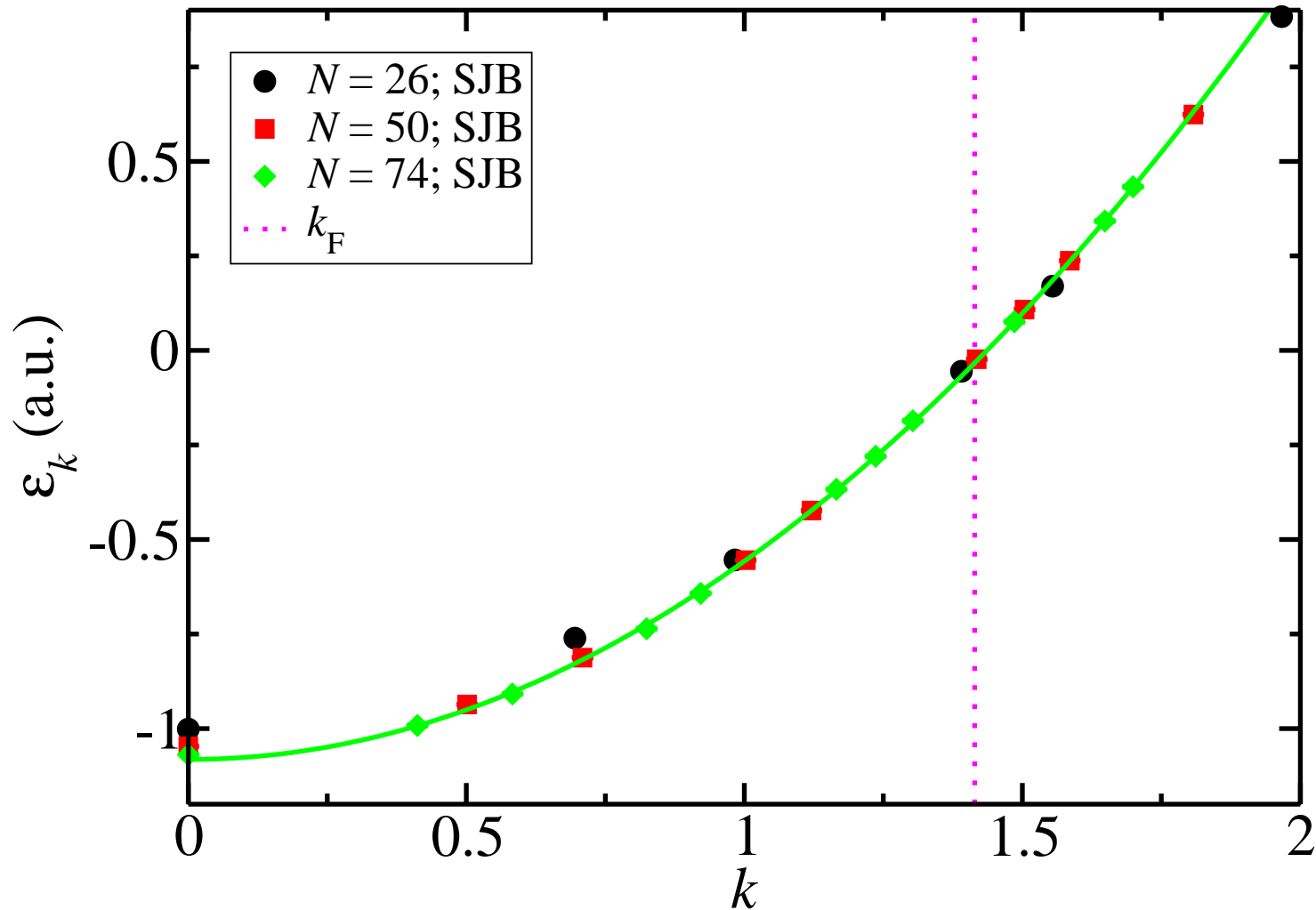
- *Single-Particle Energy Band* $\mathcal{E}_{\mathbf{k}}$ (in many-body theory):
 - **Occupied \mathbf{k}** : $\mathcal{E}_{\mathbf{k}}$ is the difference between the total closed-shell GS energy and the energy of an $(N - 1)$ -electron system with an electron removed from \mathbf{k} .
 - **Unoccupied \mathbf{k}** : $\mathcal{E}_{\mathbf{k}}$ is the difference between the energy of the $(N + 1)$ -electron system in which \mathbf{k} is occupied and the closed-shell GS energy.
- *Fermi liquid theory* justifies “single-particle” picture.
- *Quasiparticle effective mass*: $m^* = k_F / (\partial \mathcal{E}_{\mathbf{k}} / \partial k)_{k_F}$. Most important parameter in Fermi liquid theory. Lots of controversy: GW,²³ QMC²⁴ and experimental results²⁵ are inconsistent.
- DMC SP band is very sensitive to nodal surface of wave function. Less sensitive to DMC time step. Suffers some finite-size effects, although most cancel.

²³ G. F. Giuliani and G. Vignale, *Quantum Theory of the Electron Liquid*, Cambridge University Press, Cambridge (2005)

²⁴ Y. Kwon, D. M. Ceperley and R. M. Martin, Phys. Rev. B **50**, 1684 (1994); Y. Kwon, D. M. Ceperley, and R. M. Martin, Phys. Rev. B **53**, 7376 (1996).

²⁵ V. M. Pudalov *et al.*, Phys. Rev. Lett. **88**, 196404 (2002); J. Zhu *et al.*, Phys. Rev. Lett. **90**, 056805 (2003).

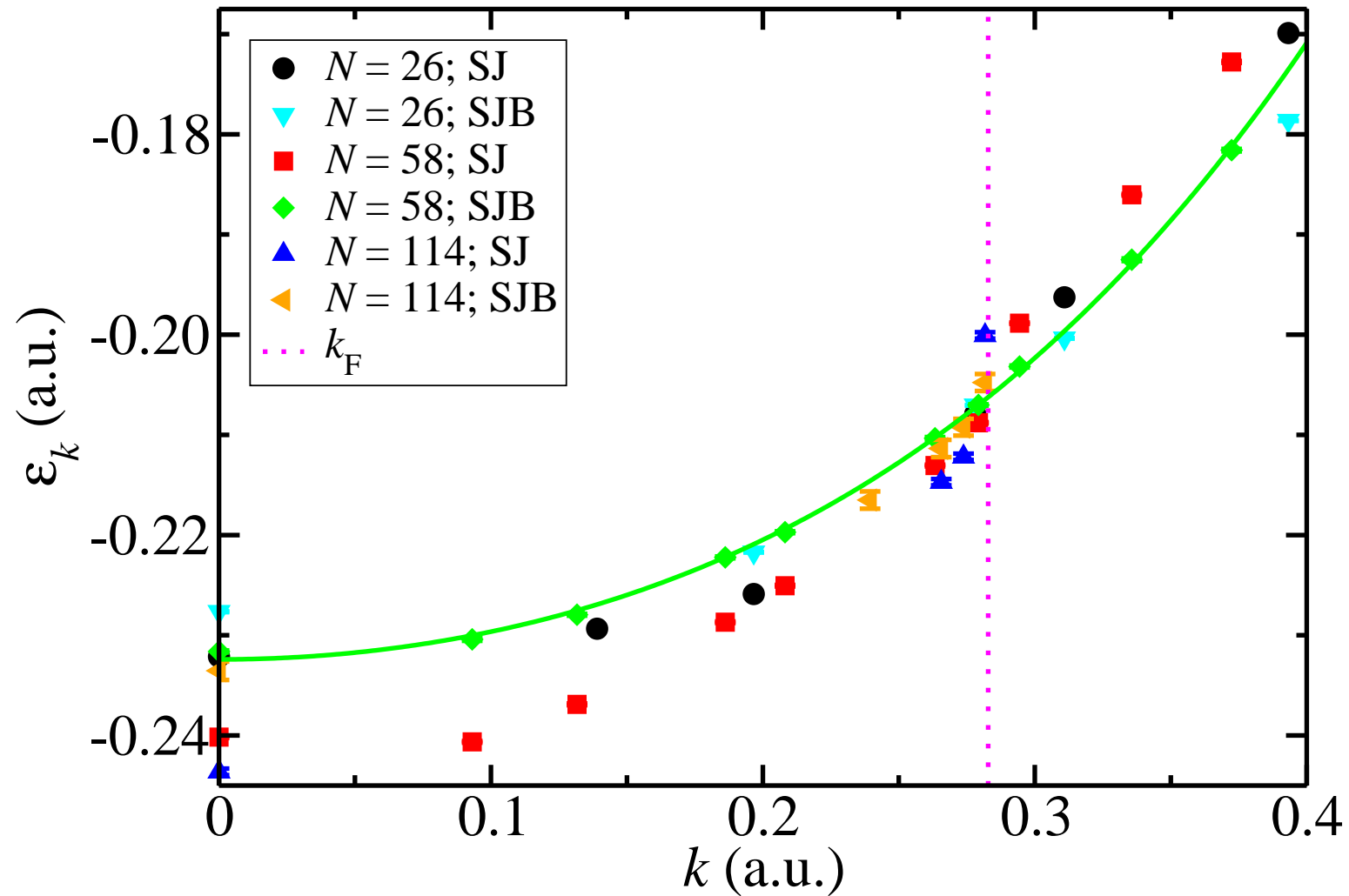
Single-Particle Energy Band (II): $r_s = 1$ a.u.



Effective mass (from fit): $m^* = 0.954$ a.u.

Fairly good agreement with earlier QMC calculation.

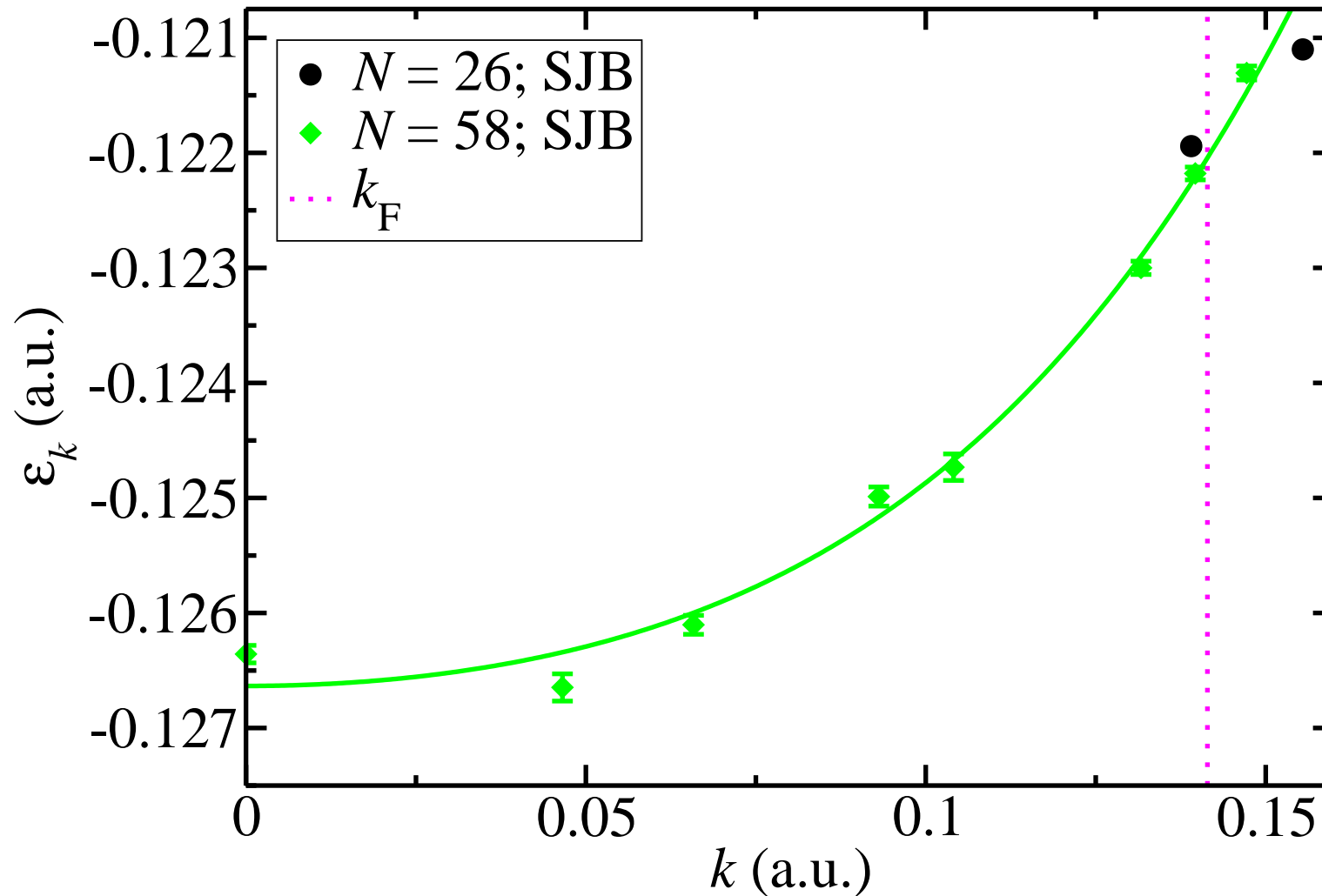
Single-Particle Energy Band (II): $r_s = 5$ a.u.



Effective mass (from fit): $m^* = 1.30$ a.u.

Energy band is very sensitive to nodal surface.

Single-Particle Energy Band (II): $r_s = 10$ a.u.



Effective mass (from fit): $m^* = 1.49$ a.u.

Significant increase in effective mass at low density, unlike earlier QMC calculations.

Conclusions

- *There is no region of stability for a ferromagnetic Fermi fluid in 2D.*
- *Wigner crystallisation occurs at $r_s = 30 \pm 1$ a.u. in 2D.*
- *Crystallisation transition is from a paramagnetic fluid to a (frustrated) antiferromagnetic triangular crystal.*
- *Transition from an antiferromagnetic to a ferromagnetic crystal at $r_s = 45 \pm 5$ a.u.*
- *Have looked for a recently proposed hybrid phase. Didn't find it. Of course there could be other types of hybrid phase. . .*
- *QMC results for contact PCF change little when wave function is improved. Suggests they are accurate. Disagreement with ladder theory.*
- *No evidence for rise in MD at Fermi edge, found in old QMC study.*
- *Calculations of energy band and effective mass are in progress.*

Acknowledgements

Financial support was received from Jesus College, Cambridge and the Engineering and Physical Sciences Research Council.



Computing resources were provided by the Cambridge High Performance Computing Service.

